Proceedings of the 35th European Safety and Reliability & the 33rd Society for Risk Analysis Europe Conference
Edited by Eirik Bjorheim Abrahamsen, Terje Aven, Frederic Bouder, Roger Flage, Marja Ylönen

doi: 10.3850/978-981-94-3281-3_ESREL-SRA-E2025-P2042-cd

Confidence Intervals in Optimized Response Surface Designs for Accelerated Lifetime Testing

Marco Arndt, M.Sc.

Institute of Machine Components, University of Stuttgart, Germany.
E-mail: marco.arndt@ima.uni-stuttgart.de

Dr.-Ing. Martin Dazer

Institute of Machine Components, University of Stuttgart, Germany.
E-mail: martin.dazer@ima.uni-stuttgart.de

Accelerated Lifetime Testing (ALT) evaluates product reliability under increased loads to expedite lifetime assessments and reduce costs. Using Response Surface Methodology (RSM) with Design of Experiments (DOE) principles enables robust multivariate exploration and modeling but faces challenges like increased prediction variance, just as in one-dimensional Wöhler models, when extrapolating to field level. Here optimized response surface designs (RSDs) are discussed that minimize extrapolation variance by strategically relocating runs while balancing model accuracy, size and test time. This paper examines Confidence Interval (CI) behavior in ALT optimized RSDs. A synthetic lifetime model generates testing times for RSDs, facilitating parameter estimation and variance analysis under efficiency-driven modifications. Numerical evaluations reveal CI properties of model responses, complemented by analysis of a central composite design (CCD) dataset to assess the impact of design manipulations. By integrating CI behavior with extrapolation variance and parameter deviations, this study advances the understanding of efficient Lifetime-RSDs in ALT.

Keywords: DOE, RSD, ALT, Reliability, Confidence Interval, Weibull-GLM

1. Introduction

Accelerated Life Testing (ALT) is a cornerstone of reliability engineering, enabling the evaluation of lifetime of products or systems under conditions where normal usage would render direct testing impractical. ALT achieves this by increasing stress levels to expedite failure mechanisms at an earlier stage, ensuring that End-of-Life (EoL) events are recorded comprehensively (uncensored) while maintaining consistent failure modes, c.f. Bertsche (2008). Here also data from tests with multiple continuous factors can be utilized to inform regression models - usually based on Generalized Linear Models considering a Weibull distribution (GLM-Weibull) and Maximum Likelihood Estimation (MLE) when multivariat testing applies, see Montgomery (2020). This however necessitates robust experimental designs that accommodate interactions and provide sound data for parameter estimation. One widely used approach is Response Surface Methodology (RSM), which offers significant advantages through experimental response surface designs (RSDs), particularly with Central Composite Designs (CCDs), c.f. Myers et al. (2016). These designs are favored for their orthogonal and rotatable properties, allowing for uncorrelated effect estimation and consistent predictive variance across the parameter space — critical for reliability modeling when the optimal testing region is uncertain. Beside interactions, CCDs excel in capturing quadratic effects, in particular when Physics of Failure (PoF) are not understood in terms of optimal reliability behavior. While CCDs may be considered as the gold standard for multivariate testing and simultaneous acceleration due to these reasons, a notable variance in prediction accuracy persists. The prediction variance increases with greater distance from the design space center when extrapolating predictions to non-accelerated field ranges. Although optimal designs might offer statistically grounded advantages as exemplarily stated by Goos and Jones (2011), no lifetime-optimized plan algorithms so far exist to significantly enhance Weibull-distributed data, c.f. Khuri (2006), Arndt and Dazer (2024a), Hinkelmann (2012). Only estimation performance metrices could potentially benefit under such approaches, while prolonged EoL test durations and the need for broad system exploration within reliability engineering remain ongoing challenges. Moreover, because the power — as a guarantee for a successful outcome of an EoL test strategy — is difficult to align with established performance indicators, the main emphasis remains on evaluating it alongside purely practical efficiency improvements. For additional details, see Rittmaier et al. (2025).

To address this limitation on both sides for exploratory and purely practical purposes, design manipulations have been proposed that typically involve repositioning CCD test runs. This aims to enhance support for the extrapolation direction without decisively altering the basic design approach and optimizing lifetime testing. Meanwhile, the main CCD shape and its structural benefits are largely retained. Importantly, these approaches maintain the total number of test runs equivalent to the baseline default CCD configuration, ensuring proper comparability and a remaining guarantee of functional fulfillment. Although the overall test duration may increase, these adjustments achieve balance by considerably enhancing predictive performance. Changes in the regressor estimates and the likelihood of detecting significant effects considering the significance level, may remain within acceptable limits, depending on the extent of the modifications. However, the consideration of confidence intervals (CI) and reliability estimates is still pending. To approach this, the present study employs a predefined system behavior, exemplifying the service life of e.g. a mechanical powertrain component for passenger vehicles, to demonstrate CI variability based on hypothetical predictions and depending on RSD optimization arrangements. Accordingly, parameter estimation, power, and variance estimation are first explained, followed by a demonstration and analysis of the employed numerical study.

2. Multivariate Reliability Modelling

A default CCD with two factors (which yields $n_F = 4$ factorial points) applies the most common configuration of $n_C = 5$ center points and an axial distance to the star points of $\alpha_D = \sqrt[4]{n_F}$, c.f. Table 1. The design center, for instance, can be set with a acceleration factor of 2.0 to 2.5 within ALT.

Assuming that a model is to be derived from each

Table 1. Default 2-factor CCD.

Type	#	x_1	x_2
factorial	1	$+1$	$+1$
	2	$+1$	-1
	3	-1	$+1$
	4	-1	-1
axial	5	α_D	0
	6	$-\alpha_D$	0
	7	0	α_D
	8	0	$-\alpha_D$
center	9	0	0
	10	0	0
	11	0	0
	12	0	0
	13	0	0

y_i failure time out of $n > k$ EoL observations in the response $\mathbf{y}$ $(n \times 1)$ based on such an RSD, the corresponding relationship can be expressed using $\mathbf{X}$ $(n \times k+1)$ containing predictor variables (stresses) and β as the vector of $j = 1, \cdots, k$ regression coefficients (effects) as follows:

$$\mathbf{y} = \mathbf{X}\beta + \varepsilon. \quad (1)$$

When modelling, here $\varepsilon \sim \mathcal{N}(0, \sigma^2)$ is a $n \times 1$ vector of independent and identically distributed (iid) random errors. Utilizing a distribution for lifetime t from the exponential family, this may be incorporated into analytical lifetime or reliability estimation via Generalized Linear Models (c.f. Myers et al. (2016)), exemplarily supplemented with a two-parameter Weibull distribution (GLM-Weibull) via the scale parameter T in

$$\ln(T) = y = \beta_0 + \sum_{j=1}^{k} \beta_j \, x_j \quad (2)$$

as follows:

$$f(t,X) = b \cdot t^{b-1}\, e^{-b\left(\beta_0+\sum_{j=1}^{k}\beta_j x_j\right)} \cdot e^{-t^b e^{-b\left(\beta_0+\sum_{j=1}^{k}\beta_j x_j\right)}}, t>0. \tag{3}$$

Finally, the Log-Likelihood Function appropriate for MLE is obtained by summing all EoL observations $t_i \sim \mathcal{W}(T;b)$ through

$$\Lambda = \ln\Big(L(t_i; b, \beta_0, \dots, \beta_k)\Big) = \sum_{i=1}^{n}\left[\ln(b) - b\cdot\Big(\beta_0+\sum_{j=1}^{k}\beta_j x_j\Big) + (b-1) \cdot \ln(t_i) - t_i^b e^{-b\left(\beta_0+\sum_{j=1}^{k}\beta_j x_j\right)}\right]. \tag{4}$$

A variety of optimization programs are suitable for finding the best estimates of maximizing factors $\hat{\theta} = \begin{bmatrix}\hat{b} & \hat{\beta}_0 & \hat{\beta}_1 & \dots \hat{\beta}_k\end{bmatrix}$ that support the GLM system equation, see also Yang (2007). Significance can be analyzed using the Likelihood-Ratio Test (LR), which is well suited to the non-normally distributed dataset. As stated by Montgomery (2020) and others, test statistic is defined by

$$\mathrm{LR} = -2\ln\left(\frac{L\big(\hat{\theta}_{(-i)}\big)}{L\big(\hat{\theta}_i\big)}\right). \tag{5}$$

Under the null hypothesis that the excluded parameter (with $\mathrm{df}=1$) in the reduced model exerts no significant influence on the target variable, LR follows a χ^2_{df} distribution with df degrees of freedom. Consequently, each p-value is given by

$$p = P\Big(\chi^2_{\mathrm{df}} \geq \mathrm{LR}\Big). \tag{6}$$

If significance level $\alpha = 0.05 > p$ applies, the parameter in question is considered significant for the model equation. Furthermore, if the power is to be measured, its value results numerically from the proportion of β identified as significant from the total number of estimates within a Monte Carlo simulation (MC). Hence, it can ultimately be translated into a reliability estimate by following:

$$\hat{R}(t,X,\hat{\theta}) = e^{-(t/\hat{T})^{\hat{b}}}. \tag{7}$$

From the inverse Fisher Information matrix (FI), Fisher CIs can be derived, which may be considered when estimating the variance of the regression model response T, failure probability $F = (1-R)$ or reliability R represented by the quantity $g = g(\theta_1, \dots, \theta_k)$:

$$\mathrm{Var}(g) \approx \sum_{i=1}^{k}\Big(\frac{\partial g}{\partial \theta_i}\Big)^2 \mathrm{Var}(\theta_i) + \sum_{i=1}^{k}\sum_{\substack{j=1\\ j\neq i}}^{k}\Big(\frac{\partial g}{\partial \theta_i}\Big)\Big(\frac{\partial g}{\partial \theta_j}\Big)\mathrm{Cov}(\theta_i,\theta_j). \tag{8}$$

Two-sided $100(1-\alpha)\%$ lower (L) and upper (U) CIs of the estimated values thus result from the $100(1-\alpha/2)\mathrm{th}$ standard normal percentile $z_{1-\alpha/2}$ in

$$[g_L, g_U] = \hat{g}_i \pm z_{1-\alpha/2}\sqrt{\hat{\mathrm{V}}\mathrm{ar}(\hat{g}_i)} \tag{9}$$

the same way as for each model response or the predicted value.

3. Study Approach

Based on the foundational elements established in Section 2 regarding multivariate reliability modeling, the prerequisites for prediction using RSDs are in place. As part of design modifications, manipulation measures and response sampling from earlier research are adopted to ensure consistency - see Figure 1 and compare Arndt et al. (2022), Arndt and Dazer (2024b) or Arndt and Dazer (2024a). These modifications include the omission of the star points $(\alpha_D, 0)$ and $(0, \alpha_D)$, as well as the removal of one of the $n_C = 5$ center runs $(0,0)$ in CCDe1 as the first manipulation stage. Next, stage CCDe2 does not discard those runs but repositions them to $(-0.8,-0.8)$, $(-1.2,-1.2)$, and $(-\alpha_D,-\alpha_D)$ in order to enhance extrapolation support towards field level. That would also be consistent with the sampled exposure boundary condition of reallocated design points according to Arndt et al. (2025), for instance when a prediction is required at $x_{Pr} = (-2.1,-1.7)$ as a hypothetical forecast point. Two objectives are thus pursued. Considering automotive or mechanical engineering products, minimal testing scope is critical due to the

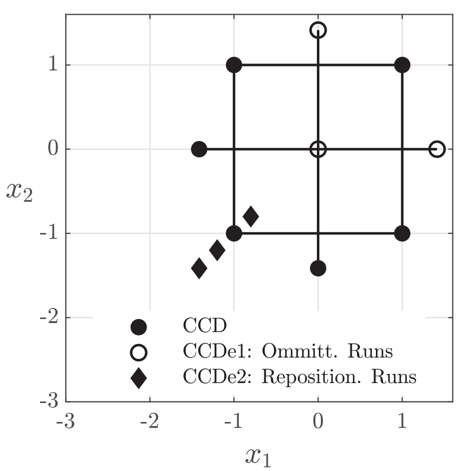

Fig. 1. CCD default configuration and design manipulations.

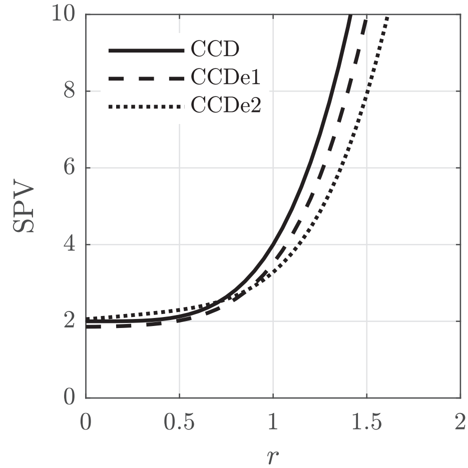

Fig. 2. EVG of RSDs.

cost of specimen. The number of design points in the most streamlined, statistically validated baseline (implemented as a default CCD) meets this requirement, and the selected modifications preserve that minimal test scope while optimizing prediction variance in the extrapolation sphere. At the same time, rotationally symmetric predictive capability is relinquished in favor of an optimized predictive strength closer to field level (compare Figure 2) and the ability to still estimate second-order effects and interactions, albeit with some trade-offs. This can also be verified in an Extrapolation-Variance Graph (EVG), which describes the Scaled Prediction Variance SPV through the directional vector $\vec{c}$ to the prediction point over the radius r using the number of experimental runs N and the design matrix X as: $v(r, \vec{c}) = Nr^2\vec{c}^T(X^TX)^{-1}\vec{c}$, compare Arndt et al. (2025)

However, those trade-offs and consequences turn observable in the estimated values of $\hat{\theta}$, the power, and the variability of $\hat{\mathrm{V}}\mathrm{ar}(g)$. Hence, the approach is to quantify these impacts numerically, either via the median or, with respect to the power, by considering the proportion of significant effects identified within $n_{\mathrm{Mc}} = 10^4$ MC iterations.

Analogously to Arndt and Dazer (2024b), here a regression model describing $\tilde{T}$ is provided first according to Equation 2 and Table 2, whereby normally distributed effects are generated through $\tilde{\beta} \sim \mathcal{N}(\beta, \sigma^2)$. This serves to take into account scatter within a fictitious, predefined physical system whose wear behavior can be measured. In addition, a failure mechanism with $b = 1.4$ is specified, from which random fictitious EoL times

$$t_{\mathrm{Mc}} \sim \mathcal{W}\big(\tilde{T}_{\mathrm{Mc}}, b\big) \tag{10}$$

are generated and assigned to the runs of the CCD, CCDe1, and CCDe2 designs each for evaluation. Note that in each MC iteration, the drawn synthetic data remain the same for all RSDs, forming a shared data basis for the MLE - compare Figure 3. Furthermore, note that in the context of this study, the focus is now directed towards reliability estimates and variance

Table 2. Synthetic Model.

Parameter	**Value**
b	1.40
β_0	10.00
β_1	-2.00
β_2	-1.00
β_{12}	1.00
β_{11}	-1.00
β_{22}	-1.00
σ	1.00

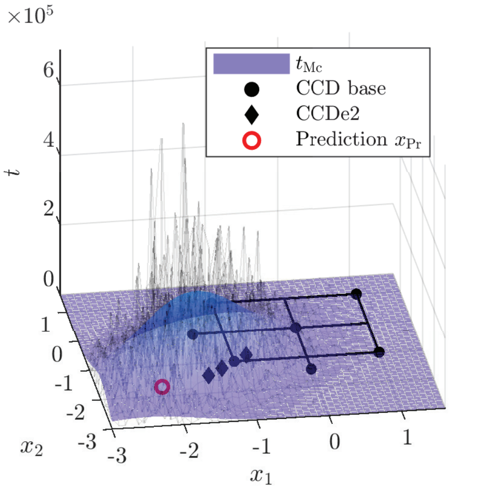

Fig. 3. Sampled t_{Mc} based on Table 2 and exemplified by CCDe2.

assessments – hence, the estimation of the shape parameter b is included here and exerts an influence, in contrast to previous contributions. This yields n_{Mc} outcomes of $\hat{\theta}_{\mathrm{Mc}}$, $\hat{p}_{\mathrm{Mc}}$-values, $\hat{T}_{\mathrm{Mc}}$, $\hat{R}_{\mathrm{Mc}}$, and $\hat{\mathrm{V}}\mathrm{ar}_{\mathrm{Mc}}(\hat{\theta}_{\mathrm{Mc}}, \hat{T}_{\mathrm{Mc}}, \hat{R}_{\mathrm{Mc}})$ per design, which are estimated according to Equation 4 by $n_{\mathrm{pat}} = 200$ patternsearch iterations optimizing the Log-Likelihood Function and analyzed via Equations 5 - 8, c.f. Section 2 and Yang (2007). The actual difference, that is, the numerically determined impact of the design variants CCD, CCDe1, and CCDe2 on the estimated system behavior and effects, is presented and interpreted in the following results section.

4. Results

The results first provide insights into the estimation deviations of the MLE $\hat{\theta}$, followed by the power values for all estimated factor-effects, compare Table 3. It is first observed that the estimated values for all applied design variants consistently overestimate the shape parameter $\hat{b}$ in the median — most significantly in the CCDe1, which has the lowest test effort in comparison. A deviation exceeding 10% from the original PoF-inspired reference model is marked with $\Updownarrow$. The estimated parameters for the main effects and interactions, on the other hand, exhibit more moderate deviations and thus align with the predefined ground truth. The quadratic effects behave differently: $\hat{\beta}_{11}$ and $\hat{\beta}_{22}$ are overestimated in their negative magnitude, almost independently of the design choice — whether default or manipulated. The power values of all estimators $\hat{\theta}_i$ consistently reach around 80% or higher.

Table 3. Numerical GLM-Weibull Estimate and Power Results. Changes indicated by $\updownarrow \leq 10\% < \Updownarrow$. power ≥ 0.80 marked with ✓.

	System	CCD	CCDe1	CCDe2
$\hat{b}$	1.40	1.96 $\Uparrow$	2.17 $\Uparrow$	1.91 $\Uparrow$
$\hat{\beta}_0$	10.00	10.04 $\uparrow$	10.04 $\uparrow$	10.03 $\uparrow$
$\hat{\beta}_1$	-1.99	-1.98 $\uparrow$	-2.06 $\downarrow$	-2.09 $\downarrow$
$\hat{\beta}_2$	-1.00	-1.00	-1.06 $\downarrow$	-1.06 $\downarrow$
$\hat{\beta}_{12}$	1.00	1.00	1.05 $\uparrow$	1.09 $\uparrow$
$\hat{\beta}_{11}$	-1.00	-1.10 $\downarrow$	-1.20 $\Downarrow$	-1.15 $\Downarrow$
$\hat{\beta}_{22}$	-0.99	-1.10 $\Downarrow$	-1.16 $\Downarrow$	-1.14 $\Downarrow$
power$_1$		0.95 ✓	0.95 ✓	0.96 ✓
power$_2$		0.83 ✓	0.84 ✓	0.85 ✓
power$_{12}$		0.76	0.79	0.85 ✓
power$_{11}$		0.86 ✓	0.85 ✓	0.87 ✓
power$_{22}$		0.86 ✓	0.86 ✓	0.88 ✓

Subsequently, the variances of the estimators as well as the resulting CIs of the regression coefficients and effect sizes are examined. Figure 4

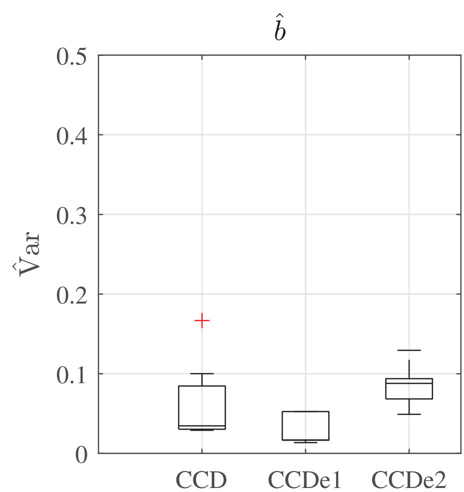

Fig. 4. Variance Variability of shape parameter $\hat{b}$ within MC Iterations per RSD.

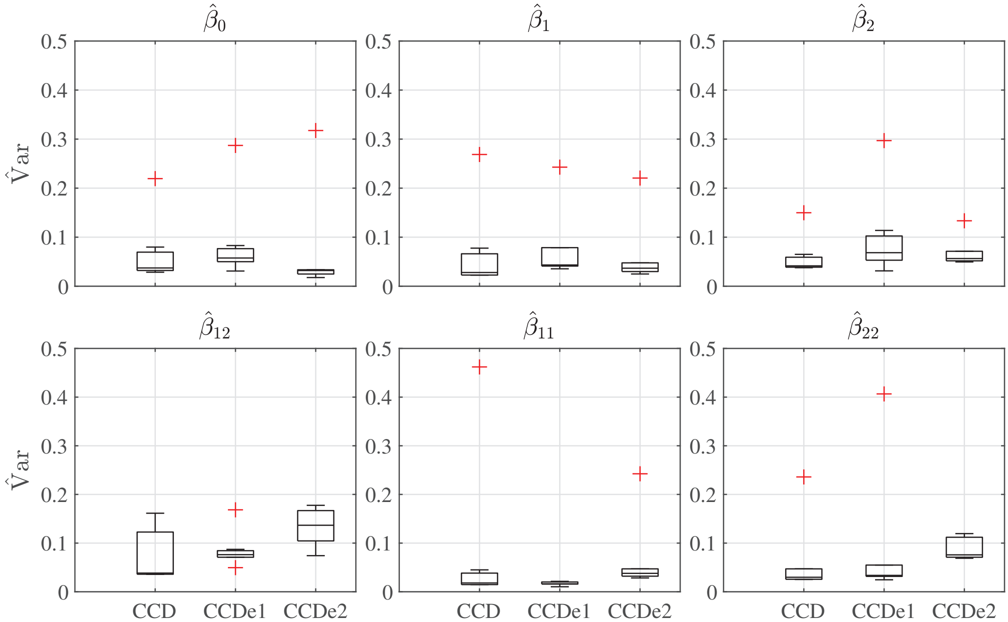

Fig. 5. Variance Variability of β_i within MC Iterations per RSD.

initially presents the boxplots of the estimated $\hat{\mathrm{V}}\mathrm{ar}(\hat{b})$ across all MC iterations, comparing the different RSDs. In addition to an outlier value ($\oplus$), the results indicate that the variability of the variances spans a comparable range but tends to be larger for CCDe2 in median, although all values remain within a moderate range below 0.1. A similar pattern emerges for the estimated regression coefficients of the GLM model, whose variance ranges are illustrated in Figure 5. In addition to certain outliers in the estimated variances derived from the FI-inverses (as discussed in Section 2), the boxplots exhibit a comparable trend. Only the interaction term and the quadratic effect of factor x_2 tend to show higher variance values for CCDe2, while the remaining variances cover similar spans - although all values remain within a relatively moderate range. This trend continues when considering the absolute confidence intervals (CIs) of the model parameters. These were determined according to Equation 9 and

$$[\theta_{i,L}, \theta_{i,U}] = \hat{\theta}_i \exp\left(\pm \frac{z_{1-\alpha/2}\sqrt{\hat{\mathrm{V}}\mathrm{ar}(\hat{\theta}_i)}}{\hat{\theta}_i}\right)$$

following the approach outlined in Yang (2007). Table 4 presents the corresponding 90% confidence intervals for $\hat{\theta}_i$. While these intervals appropriately encompass the estimates from Table 3 as well as the reference values from Table 2, the observed overestimation of the shape parameter $\hat{b}$ reveals that its reference value is positioned distinctly at the lower boundary — CCDe1 can be found to be completely beyond with CIs for $\hat{b}$. This suggests that, even when accounting for statistical confidence, the model does not adequately explain this deviation. In contrast, across all RSDs, the model parameters are consistently contained within their respective confidence intervals. Lastly, the resulting reliability functions $R(t)$ at the hypothetical prediction point x_{Pr} can be exemplarily illustrated, see Figure 6. In particular, the system reliability function is also shown, which serves as a reference while representing the actual reliability function in Figure 3. Additionally, the predicted values for the design variants CCD and CCDe1 are displayed, as well as those for CCDe2, whose behavior most closely follows the exemplary reference when accounting

Table 4. 90% CI for $\hat{\theta}_i$.

	CCD	CCDe1	CCDe2
$\hat{b}$	(1.39, 2.76)	(1.48, 3.17)	(1.37, 2.68)
$\hat{\beta}_0$	(9.73, 10.36)	(9.74, 10.35)	(9.71, 10.36)
$\hat{\beta}_1$	(-2.33, -1.69)	(-2.46, -1.72)	(-2.54, -1.72)
$\hat{\beta}_2$	(-1.38, -0.73)	(-1.50, -0.75)	(-1.56, -0.72)
$\hat{\beta}_{12}$	(0.63, 1.59)	(0.72, 1.54)	(0.78, 1.52)
$\hat{\beta}_{11}$	(-1.47, -0.82)	(-1.73, -0.83)	(-1.80, -0.74)
$\hat{\beta}_{22}$	(-1.47, -0.82)	(-1.70, -0.80)	(-1.80, -0.73)

for stochastic effects. The support of the test runs in the extrapolation direction demonstrates a positive influence through the additional information gained in parameter estimation near the target point. When considering the confidence intervals (dashed and dotted), which are included here only as supplementary information, only marginal differences due to the RSD approach can be observed. Across all estimates, these intervals are generally quite broad due to the generated test durations.

4.1. *General Findings*

With the outcome gathered so far, the following findings can be formulated:

- The chosen optimizer in the estimation algorithm consistently overestimates the shape parameter $\hat{b}$, regardless of the design being default or modified, thus systematically biasing the failure mechanism away from the predefined default model, which serves as a PoF reference.
- Regardless of the model, the estimated model parameters remain stable within a comparable range in the median.
- Additionally, they exhibit a robust and satisfactory probability of success for accurate estimation, as evidenced by power values of approximately 80% and higher, which is considered healthy according to the literature (Montgomery (2020)).
- Variances, particularly in cases of design modifications and support efforts for extrapolated predictions (CCDe2), remain at a consistent and viable level.
- The CIs are stable and acceptable in both width and position - for CCDe2 and both default setups.
- The reliability prediction benefits considerably from an optimized design setup as exemplary proposed through CCDe2.
- By opting for an efficiency-driven adaptation of the established and powerful CCD with support for the prediction point (cf. exemplary approach with CCDe2), no deterioration is achieved in any of the performance indicators and the forecasting capability is substantially improved.

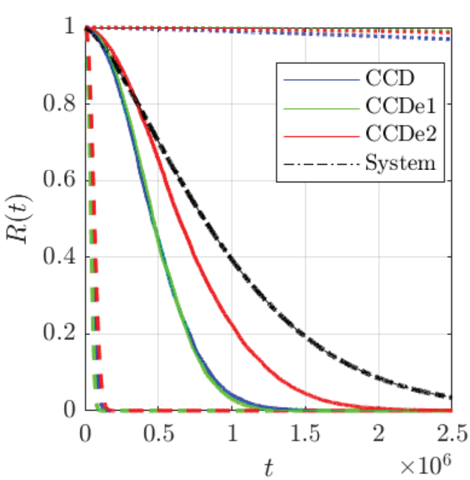

Fig. 6. Median $R(t)$ with upper and lower CI compared through CCD, CCDe1, CCDe2.

5. Conclusion

Within the scope of this study, as well as in previous research, an adapted design (CCDe2) was proposed to provide support for extrapolative predictions while maintaining the efficiency of a minimal test scope as conventionally implemented by the CCD. This was achieved by strategically shifting individual design points. At the same time, advantages such as the capability of estimating nonlinear models and generic applicability were retained. This study extends the state of research by incorporating the evaluation of variances and CIs using a numerical approach, based on the resulting median values. The results confirm the approach as viable, enabling comparisons of model estimates, power, variances, CIs, and reliability predictions. Comparisons reveal that design modifications, such as those in CCDe2, which were optimized in previous work with respect to prediction variance, are robust and comparable to both the reference model and estimates from default designs. When variance and CI evaluations are integrated into the actual reliability prediction, a strong improvement in the quality of estimates becomes apparent. As an optimization solution, the design proves to be effective and beneficial. It is therefore recommended as a superior and advantageous approach for multivariate ALT applications in EoL testing and reliability assessments.

References

Arndt, M. and M. Dazer (2024a). Characteristics of extrapolation-optimized response surface designs for multivariate reliability modelling and lifetime prediction. *Proceedings of the 17th International Conference on Probabilistic Safety Assessment and Management & Asian Symposium on Risk Assessment and Management (PSAM17 & ASRAM2024).*

Arndt, M. and M. Dazer (2024b). Investigating practical orthogonality deviations in rsm for improved predictive reliability modeling. *2024 Annual Symposium on Reliability and Maintainability (RAMS 2024).*

Arndt, M., P. Mell, and M. Dazer (2022). Generic effects of deviations from test design orthogonality on test power and regression modelling of central-composite designs. *Proceedings of the Probabilistic Safety Assessment and Management Conference 2022 (PSAM 16).*

Arndt, M., E. Rittmaier, and M. Dazer (2025). Assessing the extrapolation variance of non-orthogonal response surface designs. *2025 Annual Symposium on Reliability and Maintainability (RAMS 2025).*

Bertsche, B. (2008). *Reliability in Automotive and Mechanical Engineering: Determination of Component and System Reliability* (1st ed.). VDI-Book. Springer.

Goos, P. and B. Jones (2011). *Optimal Design of Experiments: A Case Study Approach* (1st ed.). John Wiley & Sons, Inc.

Hinkelmann, K. (2012). *Design and Analysis of Experiments - Volume 3: Special Designs and Applications* (1st ed.). John Wiley & Sons, Inc.

Khuri, A. (2006). *Response Surface Methodology and Related Topics* (1st ed.). World Scientific Publishing Co Pte Ltd.

Montgomery, D. C. (2020). *Design and Analysis of Experiments* (10th ed.). John Wiley & Sons, Inc.

Myers, R. H., D. C. Montgomery, and C. M. Anderson-Cook (2016). *Response Surface Methodology: Process and Product Optimization Using Designed Experiments* (4 ed.). Hoboken, NJ, USA: John Wiley & Sons, Inc.

Rittmaier, E., M. Arndt, and M. Dazer (2025). Analysis of statistical power of optimal experimental designs. *2025 Annual Symposium on Reliability and Maintainability (RAMS 2025).*

Yang, G. (2007). *Life Cycle Reliability Engineering* (1 ed.). Wiley series in probability and statistics. Hoboken, NJ, USA: John Wiley & Sons, Inc.